

Gripper Contacts for Part Alignment

Mike Tao Zhang, *Student Member, IEEE*, and Ken Goldberg, *Senior Member, IEEE*

Abstract — The initial resting pose of many industrial parts differs from the orientation desired for assembly. We show that it is possible to align parts during grasping using a standard parallel-jaw gripper. A solution is an arrangement of four gripper contacts that will align the part as the jaws close. We analyze toppling, jamming, accessibility, and form closure and give an $O(n^4)$ numerical algorithm to compute a set of solutions for a given n -sided polygonal part or a report that no solution exists. We have implemented the algorithm and report sensitivity data from physical experiments.

Index Terms — Robot grasping, toppling manipulation, gripper design, part feeding.

I. INTRODUCTION

“Grippers can be the most design-intensive components of an assembly system” [15]. Although grippers are widely used for automated manufacturing, assembly, and packing, designing gripper jaws is usually ad-hoc and remains a limiting factor in industrial applications. This paper proposes a new approach based on mechanics and part geometry.

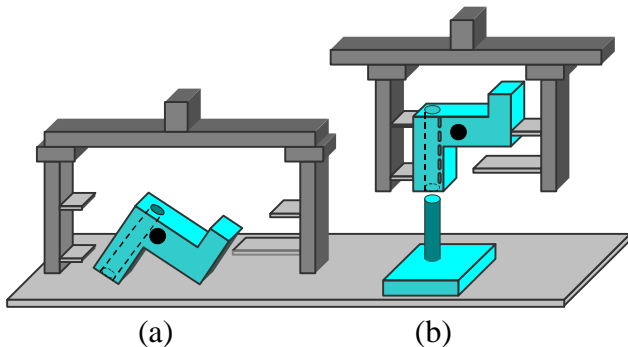


Fig. 1. Gripper contacts align the part for assembly.

Industrial parts on a flat worksurface will naturally come to rest in one of several stable orientations [12], but it is often necessary to rotate parts into different orientations for assembly. Figure 1 illustrates how parts can be aligned using a standard parallel-jaw gripper. The part is initially in

stable orientation (a); as the jaws close, the part is passively rotated into orientation (b) for assembly onto the peg. Given part geometry, we study how to compute the position of four gripper contacts. We illustrate notation in Fig. 2. During the *toppling* phase, pushing tip A' and toppling tip A make contact with the part to rotate it from the initial stable orientation to its desired orientation. During the *grasping* phase, fixturing tips B' and B make contact with the part, stop its rotation, and securely grasp it. The gripper with four jaw tips is low in cost, footprint, and weight, and can be rapidly reconfigured to handle different parts.

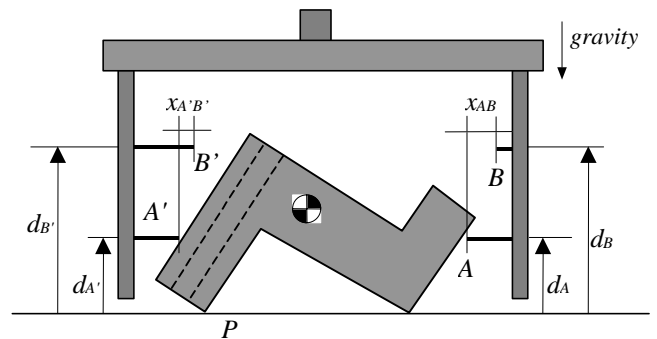


Fig. 2. Contacts A and A' rotate the part into its desired orientation. It is then grasped with contacts B and B' .

II. RELATED WORK

There is a substantial body of research on robotic grasping. Useful surveys can be found in [13], [24], [16], [26], [33], [27], [3], and [4].

Final grasp configurations can be analyzed with classical screw theory. Markenscoff *et al.* [21] prove, by infinitesimal perturbation analysis, that four (seven) hard contacts are necessary and sufficient to achieve form closure of a 2D (3D) object in the absence of friction. Trinkle [38] presents a quantitative test for form closure grasps in term of linear programming. Ponce *et al.* [28] address the problem of stable grasps of 3D parts and derive necessary and sufficient conditions for equilibrium and force-closure. Rimon and Burdick [32] provide exact decision process for immobilization based on higher order derivatives of part motion in C-space. Han *et al.* [14] formulate grasping problems as a set of convex optimization problems involving linear matrix inequalities. Liu [18] presents an $O(n^{3n/2})$ algorithm to compute all n -contact form closure grasps on a polygonal object. Van der Stappen *et al.* [34] give a polynomial-time algorithm to compute all form closure grasps on a polygonal part with at most four contacts.

M. T. Zhang is with the Department of Industrial Engineering and Operations Research, and K. Goldberg is with the Department of Industrial Engineering and Operations Research and the Department of Electrical Engineering and Computer Science, University of California, Berkeley, CA 94720 – 1777, USA. For more information, please contact: goldberg@ieor.berkeley.edu.

A number of papers consider part motion in the horizontal plane. The motion of parts during grasp acquisition is analyzed by Mason [22], who studies push mechanics as a role of passive compliance in grasping and manipulation. Erdmann and Mason [9] explore the use of motion strategies to reduce uncertainty in the location of objects. They describe a systematic algorithm for sensorless manipulation to orient parts using a tilting tray. Brost [6] analyzes the mechanics of the parallel-jaw gripper showing that it is possible to align parts using passive pushes and squeeze mechanics. Goldberg [11] proves that a modified parallel-jaw gripper can orient any polygon up to symmetry by a sequence of normal pushes. Akella *et al.* [2] introduce a minimalist manipulation method to feed planar parts using a one-joint robot over a conveyor belt. Qiao and her colleagues apply the concept of attractive regions to peg-in-hole insertion operations [29] and to pushing and grasping in 3D C-spaces [30].

Several authors address motion of parts in the vertical (gravitational) plane during grasping. Erdmann [10] studies nonprehensile manipulation in C-space and develops an algorithm for sensorless part orienting. Abell and Erdmann [1] study how a planar polygon can be rotated while stably supported by two frictionless contacts. Zumel and Erdmann [44][45] analyze nonprehensile manipulation using two palms jointed at a central hinge. Rao *et al.* [31] give an analysis for picking up polyhedral parts using 2 hard-point contacts with a pivoting bearing, allowing the part to pivot under gravity to rotate into a new configuration. Blind *et al.* [5] present a “Pachinko”-like device to orient polygonal parts in the vertical plane. It consists of a grid of retractable pins that are programmed to bring the part to a desired orientation as the part falls. Moll and Erdmann [25] orient parts by dropping them on specially designed surfaces. They adjust the shape of the surface and the drop height to obtain a combination that yields a minimal entropy distribution of the part’s final orientation.

Perhaps closest to the current paper, which addresses multiple-contact toppling and grasping, is the work of Trinkle *et al.* [36][37], which analyzes lifting parts off a work-surface using a planar gripper with two pivoting jaws. They generate *liftability regions* corresponding to the contacts causing the object to: slide, jam, break either of two contacts with the surface, or break both contacts with the surface. One important difference is that we focus on part alignment using only translational motion of gripper jaws. Kaneko *et al.* [17] derive a sufficient condition to move an enveloped part using a set of torque commands. To efficiently predict the dynamic behavior of a grasp, Song *et al.* [35] provide a hybrid approach by switching to a compliant model when a rigid body model has no unique solution.

Wallack and Canny [39] develop an algorithm for planning planar grasp configurations using a modular vise. Brown and Brost [7] turn the vise upside down to form a modular parallel-jaw gripper. Each jaw consists of a regular grid of precisely positioned holes. By properly locating (inserting) four pins on each grid, the object can be grasped reliably in the desired orientation. They give an efficient algorithm for computing optimal positions for pins

depending on a planar fixture model and additional 3-D geometry analysis.

Our work is also motivated by recent research in toppling manipulation. Zhang and Gupta [41] study how parts can be reoriented as they fall down a series of steps. The authors derive the condition for toppling over a step and defined the transition height, which is the minimum step height to topple a part from a given stable orientation to another. Yu *et al.* [40] estimate the center of mass (COM) of objects by toppling. Lynch [19] [20] derives sufficient mechanical conditions for toppling parts on a conveyor belt in term of constraints on contact friction, location, and motion. For pin design, we introduce a set of geometric functions to describe the mechanical property of toppling [42].

The approach described in this paper is consistent with the guidelines proposed by Causey and Quinn [8] for the design of grippers for manufacturing: include functionality in gripper jaws, use jaws to align parts, and design for proper gripper-part interaction. We combine toppling mechanics with an analysis of jamming, accessibility, and form closure in the gravitational plane. A preliminary report on this approach appeared in [43].

III. PROBLEM DEFINITION

Given a part, we want four contacts that will rotate it into a desired orientation and grasp it securely. The input is: the vertices of an n -sided convex projection of an extruded polygonal part, its center of mass (COM), initial and desired orientations, a vertex clearance radius ϵ , and bounds on the part-surface friction coefficient $[0, \mu_{s_max}]$ and on the part-gripper friction coefficient: $[\mu_{t_min}, \mu_{t_max}]$. The output of the algorithm is a report that no solution can be found or a set of solutions, each given as the position of four jaw tips (see Fig. 2).

We assume that the part and the gripper are rigid, and that the part’s geometry, the location of its COM, and the position of the jaws are known exactly. We also assume that inertial effects are negligible during part motion. Without loss of generality, we assume that the part will be rotated counter-clockwise. Jaw tips for clockwise rotation can be computed using a mirror image of the part.

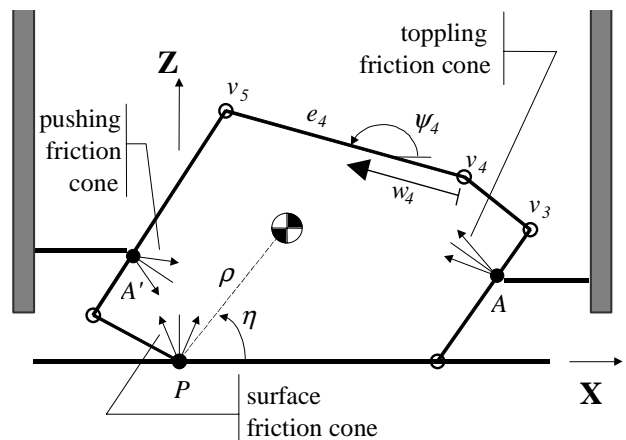


Fig. 3. Convex hull of the part in Fig. 2.

Fig. 3 shows the convex hull of the part sitting on a flat work-surface in its stable orientation. During the toppling phase, the toppling tip A and pushing tip A' make contact with the part and rotate it counterclockwise, maintaining contact between the work-surface and pivot point P . We define a frame originating at P with X-axis on the surface pointing right and Z-axis pointing up. This frame translates to the right as the part is pushed.

Consider the part at its initial orientation. Its COM is a distance ρ from P and an angle η from the +X direction. Starting from P , we consider each edge of the part in counter-clockwise order: e_1, e_2, \dots, e_n . The edge e_i , with vertices v_i at (x_i, z_i) and v_{i+1} at (x_{i+1}, z_{i+1}) , is in direction ψ_i from the +X axis. Let w_i be the distance along edge e_i as shown in Fig. 3. Any point on e_i can be expressed as $(x_i + w_i \cos \psi_i, z_i + w_i \sin \psi_i)$.

Let θ denote the rotational angle of the part as measured from the X-axis. Initially $\theta = 0$; θ_d is the part's desired orientation and θ_l is its next stable orientation in the counter-clockwise direction. We assume $\theta_d < \theta_l$. We say an edge e_k is *visible* if it can be seen from +X direction; *invisible*, otherwise. Thus, e_k is visible if $0 < \psi_k + \theta < \pi$; e_k is invisible if $\pi < \psi_k + \theta < 2\pi$. Note that A can only make contact with visible edges and that A' can only make contact with invisible edges.

Our analysis involves the graphical construction of a set of geometric functions that represent the mechanics of part alignment including the radius function, the vertex function, the rolling function, and the jamming function. These functions are dependent on θ and map from part orientation to height: $S^1 \rightarrow \mathfrak{R}^+$, where S^1 is the set of planar orientations. We study the toppling phase and the grasping phase in the following two sections.

IV. TOPPLING PHASE

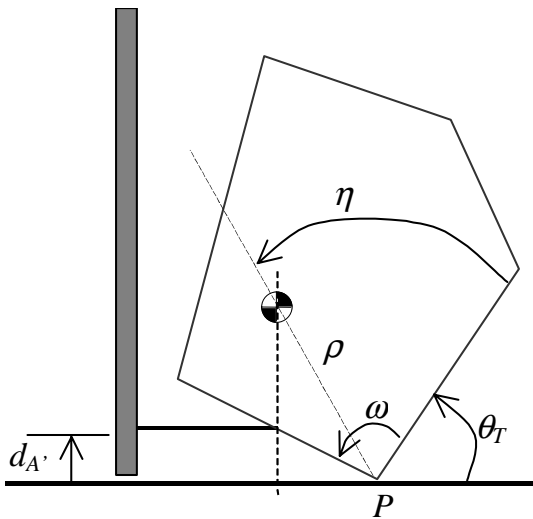


Fig. 4. θ_T : critical transformation angle from rolling sub-phase to setting sub-phase.

We divide the toppling phase into two sub-phases: *rolling* and *settling*, where the COM is to the right and left of the vertical line through the pushing tip A' , respectively. Let θ_T denote the critical transition angle where the COM is directly above A' . As shown in Fig. 4, let ω denote the interior angle of the part at pivot point P . We obtain Equation (1) through geometric construction and solve it for θ_T .

$$d_A \cdot \tan(\theta_T + \omega) = \rho \cos(\eta + \theta_T). \quad (1)$$

The radius function, $R(\theta)$, is the height of the COM as the part is rotated [22]. The local minima of the radius function correspond to stable orientations of the part. Each vertex of the part defines a vertex function, $V_i(\theta)$, which gives the height of vertex i as the part rotates. The vertex functions define which part edge a jaw tip at a given height will touch. Given d_A , the range of friction coefficients, and the toppling tip A in contact with edge e_i , the rolling function $H_i(\theta)$ is the minimum height of A guaranteed to cause the part to rotate at orientation θ . $H_i(\theta)$ is defined in the range $[0, \theta_T]$. Given d_A , the range of friction coefficients, and A in contact with edge e_i , the jamming function $J_i(\theta)$ gives the minimum height of A that is guaranteed not to cause jamming.

Below, we initially assume that part-surface and part-gripper friction coefficients are given precisely. We then relax this assumption to define $H_i(\theta)$ and $J_i(\theta)$ given bounds on μ_s and μ_l .

A. Rolling Sub-Phase

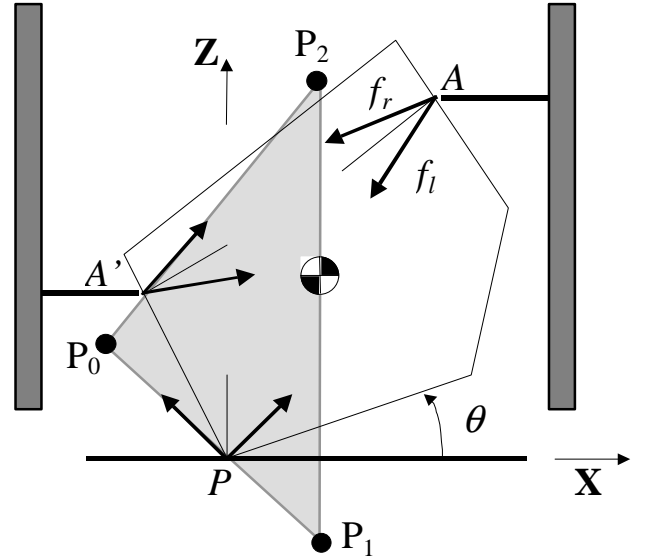


Fig. 5. Rolling conditions ($\pi > \omega + \theta > \pi/2$).

During the rolling sub-phase, the part has three contacts: A' , A , and P . The part rotates and translates relative to these contacts. The system of forces on the part, including the contact force at the work-surface, the contact force at the tips, and the part's weight, must generate a

positive moment on the part with respect to pivot point P . The contact force at P is along the left edge of the surface friction cone, but the direction of the contact force at A' depends on angle $\omega + \theta$.

Consider the case where $\pi > \omega + \theta > \pi/2$. Rotation causes the contact between the part and A' to move away from P . Thus the contact force at A' is along the left edge of the pushing friction cone.

Following the graphical method of Mason [23], we construct a triangle $P_0P_1P_2$ as shown in Fig. 5. Each edge of the triangle corresponds to a contact force or gravity force. With the coordinate frame as defined above, with origin at pivot point P , P_0 is at (x_{p0}, z_{p0}) , which is the intersection of the left edge of the surface friction cone and the left edge of the pushing friction cone. P_1 is at (x_{p1}, z_{p1}) , which is the intersection of the vertical line through the COM and the left edge of the surface friction cone. P_2 is at (x_{p2}, z_{p2}) , which is the intersection of the vertical line through the COM and the left edge of the pushing friction cone. Let r_{01} denote the line segment between P_0 and P_1 and let $|r_{01}|$ denote its length. We denote r_{02} , r_{12} , $|r_{02}|$, and $|r_{12}|$ similarly. Thus we have:

$$x_{p0} = t - |r_{01}| \sin \alpha_s, \quad (2)$$

$$z_{p0} = -t/\mu_s + |r_{01}| \cos \alpha_s, \quad (3)$$

$$x_{p1} = t, \quad (4)$$

$$z_{p1} = -t/\mu_s, \quad (5)$$

$$x_{p2} = t, \quad (6)$$

$$z_{p2} = \frac{\frac{d_A}{\tan \varphi} - t}{\tan(\varphi + \alpha_i)}, \quad (7)$$

$$\text{where } t = \rho \cos(\eta + \theta), \varphi = \omega + \theta \text{ and } (8)$$

$$|r_{01}| = \frac{(z_{p2} + \frac{t}{\mu_s}) \sin(\varphi + \alpha_i)}{\sin(\varphi + \alpha_i - \alpha_s)}. \quad (9)$$

The locations of P_0 , P_1 , and P_2 are a function of θ . As θ increases, P_1 shrinks to P along r_{01} , r_{02} sweeps counterclockwise, and P_2 moves up while r_{12} remains parallel to the Z -axis. Triangle $P_0P_1P_2$ exists if and only if $\omega + \theta + \alpha_i < \pi$, i.e. $\theta < \pi - \omega - \alpha_i$.

Toppling is guaranteed if every force in the toppling friction cone makes a positive moment about every point in the $P_0P_1P_2$ triangle. For all forces in the toppling friction cone to generate a positive moment about the triangle, the left edge of the friction cone must pass above the triangle; all other vectors in the friction cone will pass higher. We denote the vector at the left edge of the toppling friction cone as f_l and the right edge as f_r . We find the height of A sufficient to roll the part by projecting lines from P_0 , P_1 , and P_2 along angle f_l into the edge contacting A . The maximum of these projections is the minimum height of A sufficient to roll the part.

Let $w_{i,2}$ denote the distance from vertex v_i to A along edge e_i where the left edge of the toppling friction cone passes exactly through point P_2 . Let X_i and Z_i denote the location of vertex v_i after the part undergoes pure rotation

by angle θ , i.e., $X_i = x_i \cos \theta - z_i \sin \theta$ and $Z_i = x_i \sin \theta + z_i \cos \theta$. We can show through geometric construction that:

$$w_{i,2}(\theta) = \frac{Z_i - z_{p2} - (X_i - x_{p2}) \tan \gamma_{il}}{\cos \xi_i \tan \gamma_{il} - \sin \xi_i} \quad (10)$$

where $\xi_i = \theta + \psi_i$ and $\gamma_{il} = \psi_i + \pi/2 + \alpha_i + \theta$.

The distances $w_{i,0}$ and $w_{i,1}$ are defined similarly, where the left edge of the toppling friction cone intersects P_0 and P_1 respectively.

The rolling function, $H_i(\theta)$, is based on $w_i(\theta)$ that is $\max(w_{i,0}(\theta), w_{i,1}(\theta), w_{i,2}(\theta))$ in the rolling region $0 < \theta < \theta_T$. $w_i(\theta)$ can be shown to be:

$$w_i = \begin{cases} w_{i,2} & 0 < \theta < \theta_m \text{ and } \psi_i < \omega \\ w_{i,0} & 0 < \theta < \theta_m \text{ and } \psi_i \geq \omega \\ \infty & \text{otherwise} \end{cases}, \quad (11)$$

where $\theta_m = \min(\theta, \pi - \omega - \alpha_i)$. Thus, the rolling function within $0 < \theta < \theta_T$ is given by:

$$H_i(\theta) = \begin{cases} H_i^*(\theta) & V_i(\theta) \leq H_i^*(\theta) \\ 0 & V_i(\theta) > H_i^*(\theta) \end{cases}, \quad (12)$$

$$\text{where } H_i^*(\theta) = Z_i + w_i \sin \xi_i. \quad (13)$$

Following the same methodology, we find $H_i(\theta)$ under the condition $\pi/2 > \omega + \theta > 0$.

Fig. 6 illustrates function $R(\theta)$, $H_2^*(\theta)$, $V_2(\theta)$ and $V_3(\theta)$ for the part in Fig. 3 with $\alpha_t = 5^\circ$, $\alpha_s = 10^\circ$ and $d_A = 9$. The kink ($\theta = 37^\circ$) of $R(\theta)$ represents the orientation where e_6 is on the surface. At a certain angle θ , any A at height h will instantaneously rotate the part if $\max(H_2(\theta), V_2(\theta)) < h < V_3(\theta)$. The toppling function indicates that A can roll the part at any contact on e_2 when $0 < \theta < 20^\circ$.

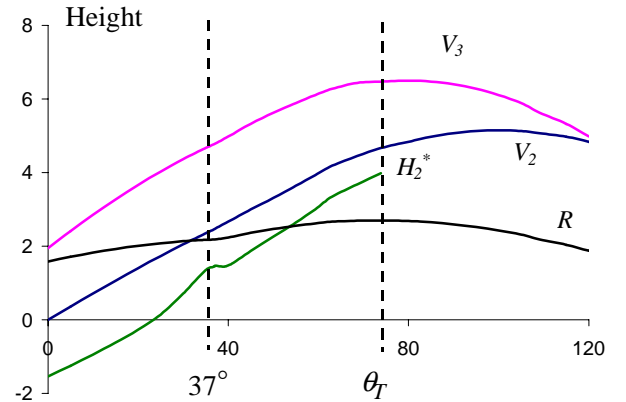


Fig. 6. Vertex functions and rolling function.

B. Settling Sub-Phase

For cases where the part's center of mass crosses over the vertical line through the pushing tip A' , the part will also rotate due to gravity in the settling sub-phase. To avoid jamming during settling, we construct another geometric function.

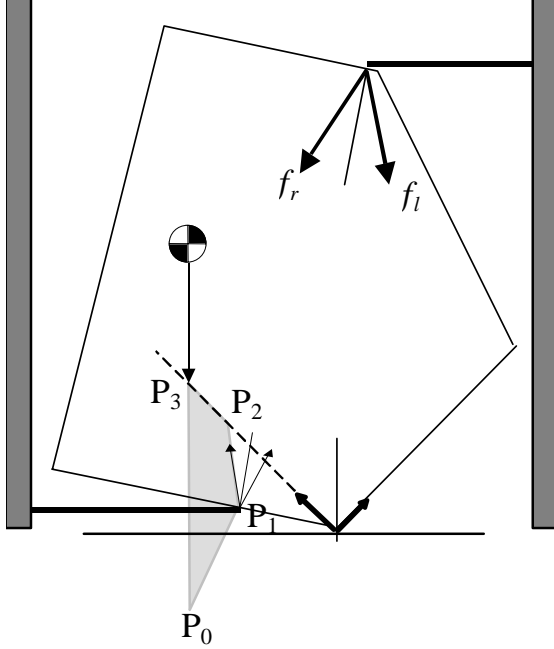


Fig. 7. Jamming conditions.

The jamming function depends on the quadrilateral $P_0P_1P_2P_3$ that is constructed as shown in Fig. 7. P_0 is at (x_{p0}, z_{p0}) , which is the intersection of the vertical line through the part's COM and the right edge of the pushing friction cone. P_1 is the pushing tip at (x_{p1}, z_{p1}) . P_2 is at (x_{p2}, z_{p2}) , which is the intersection of the left edge of the pushing friction cone and the left edge of the surface friction cone. P_3 is at (x_{p3}, z_{p3}) , which is the intersection of the vertical line through the part's COM and the left edge of the surface friction cone.

Thus, we have:

$$x_{p0} = t, \quad (14)$$

$$z_{p0} = d_A - \frac{d_A \tan \varphi - t}{\tan(\alpha_t - \varphi)}, \quad (15)$$

$$x_{p1} = d_A \tan \varphi, \quad (16)$$

$$z_{p1} = d_A, \quad (17)$$

$$x_{p2} = \frac{-d_A \cos \alpha_t \sin \alpha_s}{\sin \varphi \sin(\varphi + \alpha_t - \alpha_s)}, \quad (18)$$

$$z_{p2} = \frac{d_A \cos \alpha_t \cos \alpha_s}{\sin \varphi \sin(\varphi + \alpha_t - \alpha_s)}. \quad (19)$$

$$x_{p3} = t, \quad (20)$$

$$z_{p3} = -t/\mu_s. \quad (21)$$

Jamming may occur if any force in the toppling friction cone makes a negative moment about the quadrilateral

$P_0P_1P_2P_3$; therefore f_l determines the minimal height of A at which jamming may occur.

Similar to our analysis of the rolling function, we obtain $w_{i,0}(\theta)$, $w_{i,1}(\theta)$, and $w_{i,2}(\theta)$. When $\theta > \pi - \omega - \alpha_t + \alpha_s$, quadrilateral $P_0P_1P_2P_3$ doesn't exist and $w_i(\theta)$ is ∞ . When $\theta < \pi - \omega - \alpha_t + \alpha_s$, $w_i(\theta)$ is $\min(w_{i,0}(\theta), w_{i,1}(\theta), w_{i,2}(\theta))$ and can be shown to be:

$$w_i = \begin{cases} w_{i,0} & \psi_i < \omega - 2\alpha_t \text{ and } \theta_t < \theta < \theta_{32} \\ w_{i,1} & \omega - 2\alpha_t \leq \psi_i \leq \omega \text{ and } \theta < \theta_{32} \\ w_{i,2} & \omega < \psi_i \text{ and } \theta < \theta_{32} \\ w_{i,3} & \theta_{32} \leq \theta \leq \theta_d \end{cases} \quad (22)$$

$$\text{where } \theta_{32} = \pi - \alpha_t - \psi_i. \quad (23)$$

The jamming function, $J_i(\theta)$, with $\theta_t < \theta < \theta_d$ is given by:

$$J_i(\theta) = \begin{cases} J_i^*(\theta) & V_i(\theta) \leq J_i^*(\theta) \\ 0 & V_i(\theta) > J_i^*(\theta) \end{cases}. \quad (24)$$

$$\text{where } J_i^*(\theta) = Z_i + w_i \sin \xi_i. \quad (25)$$

Given θ and d_A , jamming is guaranteed not to occur if A makes contact with edge e_i and the toppling tip A is higher than $J_i(\theta)$.

C. Bounded Friction Coefficients

In the previous section we assumed exact friction values were given. In this section we relax that assumption and derive the rolling and jamming functions given upper and lower *bounds* on the friction coefficients.

For each value of θ , the geometric functions can take on a range of values depending on the range of friction coefficients. To guarantee toppling for all the friction values in the range, we take the maximum values of $H_i(\theta)$ or $J_i(\theta)$ over the given bounds. At each rotational angle θ , the maximum $H_i(\theta)$ or $J_i(\theta)$ corresponds to the *critical friction coefficients* denoted by μ_s^* and μ_t^* . We first consider the functions at each rotational angle θ to derive μ_s^* ; then we find μ_t^* for given μ_s^* and θ .

As illustrated in Fig. 5, P_0 moves up along r_{02} as μ_s decreases. Then, $w_{i,0}$ decreases while $w_{i,2}$ remains unchanged. Therefore $H_i(\theta)$ is guaranteed not to increase as μ_s decreases. It is sufficient to consider only the upper bounds of μ_s , i.e. $\mu_s^* = \mu_{s,max}$, to get the maximal $H_i(\theta)$ over the given range of μ_s .

As illustrated in Fig. 7, P_3 moves up along r_{03} and P_2 moves up along r_{12} as μ_s decreases. Therefore, quadrilateral $P_0P_1P_2P_3$ expands and $J_i(\theta)$ is guaranteed not to increase as μ_s decreases. It is sufficient to consider only the upper bound of μ_s , i.e. $\mu_s^* = \mu_{s,max}$, to get the maximal $J_i(\theta)$ over the given range of μ_s .

Given θ and $\mu_s^* = \mu_{s,max}$, the rolling function is a function of μ_t . In Fig. 5, P_2 moves down along r_{12} as μ_t decreases. Therefore, $w_{i,2}$ decreases and $\mu_t^* = \mu_{t,max}$ for $\psi_i < \omega$ (where w_i is determined by $w_{i,2}$). But P_0 moves up along

r_{01} as μ_t decreases, so we need to determine μ_t^* for $\psi_i > \omega$ (where w_i is determined by $w_{i,0}$). We apply binary search to the given range of μ_t for maximal w_i , which corresponds to μ_t^* .

In Fig. 7, P_2 moves down along r_{23} and P_0 moves down along r_{03} as μ_t decreases. Therefore, quadrilateral $P_0P_1P_2P_3$ expands and $J_i(\theta)$ is guaranteed not to increase as μ_t decreases. It is sufficient to consider only the upper bound of μ_s , i.e. $\mu_t^* = \mu_{t,max}$, to get the maximal $J_i(\theta)$ over the given range of μ_s .

An example is illustrated in Fig. 8. The part is defined by the vertices at (0,0), (51.2, 0), (64.1, 57.2), (37.5, 96.2), (-32.2, 44.6), and COM at (21.9, 42.3). The part is initially in stable orientation (a) and we desire to rotate it 25° into final orientation (b) for assembly.

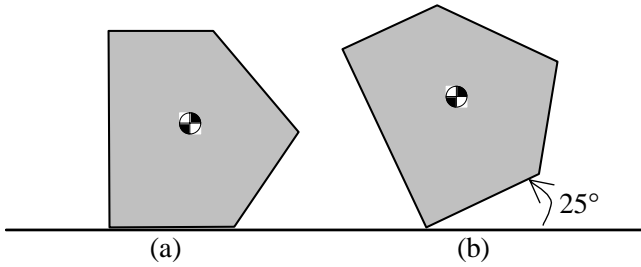


Fig. 8. An example: part alignment.

Fig. 9 shows H_3 as the function of μ_t and θ given $d_A = 5$ and $\mu_s^* = 0.17$.

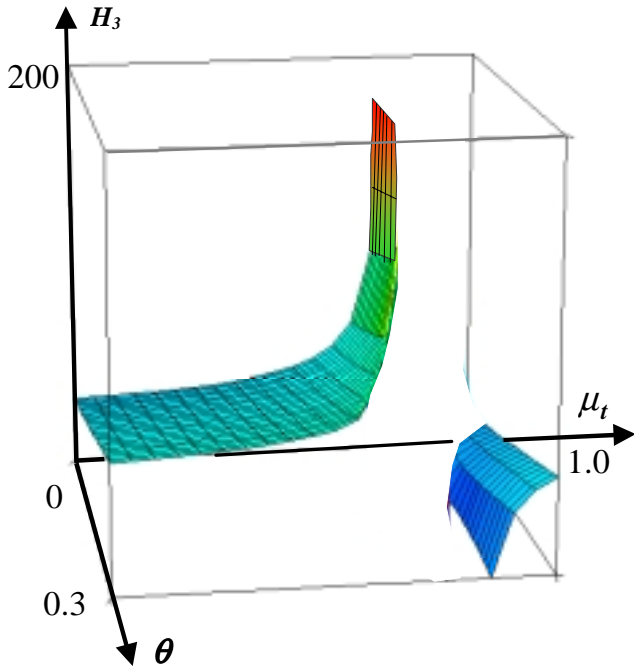


Fig. 9. Rolling function as the function of rotational angle θ and contact friction coefficient μ_t .

We slice the surface in Fig. 9 at discrete values of the rotational angle. At $\theta = 10^\circ$, Fig. 10 shows H_3 as a function

of μ_t . If $\mu_{t,max} < \mu_t$ or $\mu_{t,min} > \mu_t$, H_3 is a monotonically increasing function of μ_t ; therefore $\mu_t^* = \mu_{t,max}$. Otherwise H_3 goes to infinity. We use numerical search to find μ_t^* .

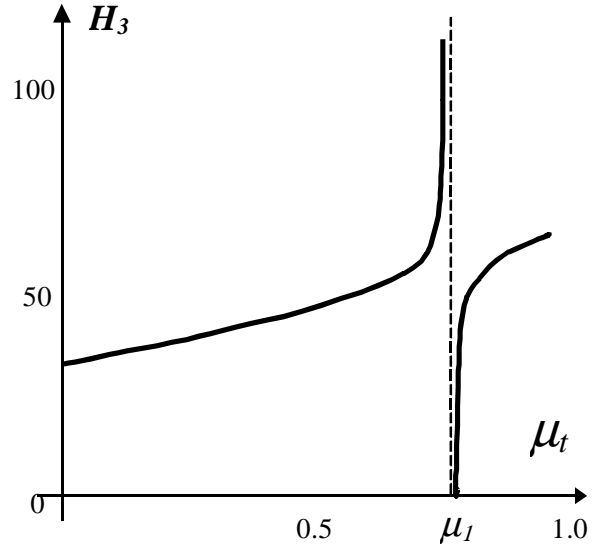


Fig. 10. Rolling function as the function of contact friction coefficient μ_t at each rotational angle θ .

We find $H_i(\theta)$ and $J_i(\theta)$ over the range of μ_s and μ_t by determining μ_s^* and μ_t^* at each θ , where $\mu_s^* = \mu_{s,max}$ for both functions and $\mu_t^* = \mu_{t,max}$ for $J_i(\theta)$. We then find μ_t^* for $H_i(\theta)$ using binary search.

D. Toppling Function

The toppling function is a vector function that combines the vertex functions, the rolling functions, and the jamming functions for the visible edges. The rolling functions and the jamming functions correspond to μ_s^* and μ_t^* at each θ . From the toppling function, the height of the toppling tip, which is capable of rotating the part to the desired orientation, can be determined or shown to be non-existent.

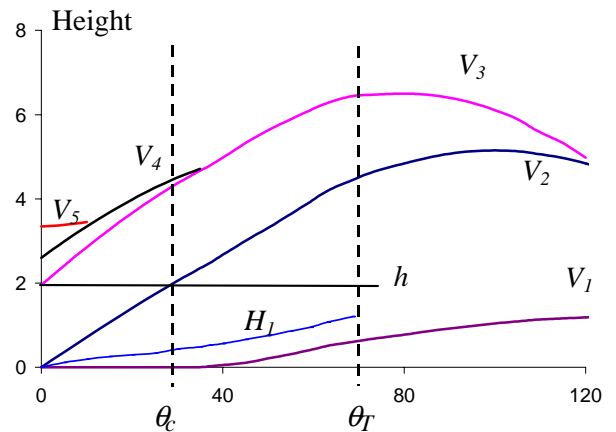


Fig. 11. Toppling function.

Fig. 11 illustrates the toppling function for the convex part in Fig. 3. We consider the toppling tip at height h (shown as height = 2 in the figure). θ_c is the critical rotation angle where h intersects V_2 , where contact A will move from e_2 to e_1 . θ_T is the critical condition where the center of mass is exactly above the pivot point. H_1 is the rolling function, which gives the minimum height of A that is in contact with e_1 . H_1 is bounded by V_1 and V_2 and is truncated where it intersects them. Since h is above H_1 , a toppling tip at height h will rotate the part from a stable initial orientation with $\theta = 0$ to $\theta = \theta_T = 71^\circ$.

A toppling tip at height h will achieve this if we can draw a horizontal line corresponding to height h in the toppling function beginning at $\theta = 0$ and ending at θ_d with the following characteristics:

- 1: $h > H_i(\theta)$, if $V_i(\theta) < h < V_{i+1}(\theta)$;
- 2: $h > J_i(\theta)$, if $V_i(\theta) < h < V_{i+1}(\theta)$;
- 3: $h < \max_i (V_i(\theta))$, if $\theta < \theta_T$.

where i is the index for the visible edges.

The first two criteria are satisfied when the toppling tip is above both the rolling function and the jamming function of the edge it contacts. When h crosses a vertex function, the part switches contact edges and then h must be above the rolling function and the jamming function for the new edge. The third criterion is that the toppling tip must not lose contact with the part by passing over it during the rolling sub-phase.

From the toppling function we can determine that the toppling tip at $d_A = h = 2$ will topple the part to θ_T .

V. GRASPING PHASE

During toppling, the part is constrained by three contacts: the toppling tip A , the pushing tip A' and the pivot point P on the work-surface. Once the part has been rotated to the desired orientation θ_d , the fixturing tips, B and B' , must terminate its rotation and achieve a form closure grasp with A and A' . We consider accessibility constraints first and then we consider form closure.

A. Accessibility

The accessibility constraints insure that B and B' do not collide with the part before it reaches its desired orientation. The accessibility constraint will limit the possible heights of B and B' for given $d_{A'}$ and d_A .

To insure accessibility from B , the point on the part at height d_B can only move towards tip B . A similar condition applies for fixturing tip B' . The *inaccessible range* shown in Fig. 12 indicates heights of B that would collide with the part before its desired orientation.

To compute the inaccessible range for B , we note that as the part rotates, the horizontal velocity of points on the part edges relative to tip A can be positive, negative and zero. There may be a point on each visible edge that has zero velocity as the part rotates through angle θ . Let B_θ be this point on edge e_j and h_θ be its height. Below h_θ , the

relative velocity of the points on e_j is positive and B_θ moves towards tip B ; above h_θ , the relative velocity is negative and B_θ moves away from tip B . The accessibility constraint requires $d_B \leq h_\theta$ for all visible edges at all θ .

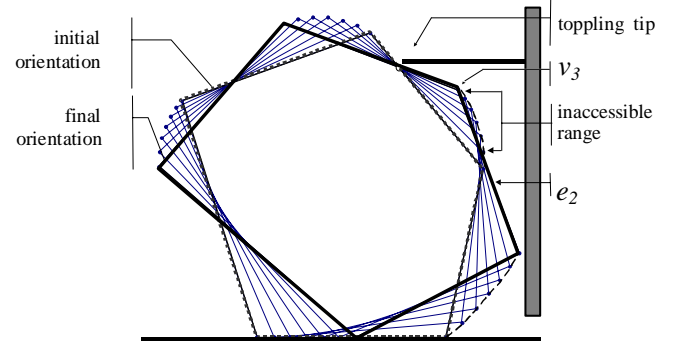


Fig. 12. Rotation of a part relative to the toppling tip A . Dotted/solid lines indicate the initial/final orientation of the part and dashed lines represents the motion trajectory of vertices.

To solve for h_θ we derive an expression for the horizontal distance between A and B_θ using the fact that the part is constrained by A and P :

$$x_\theta = X_j - X_i + \frac{d_B - Z_j}{\tan \xi_j} - \frac{d_A - Z_i}{\tan \xi_i}, \quad (29)$$

where i and j are the indexes of the edges in contact with A and B respectively and ξ_i is as defined in Equation (10). To find the point with zero horizontal velocity relative to tip A , we take the derivative of x_θ with respect to θ :

$$\frac{dx_\theta}{d\theta} = Y_i - \frac{d_A - X_i}{\tan \xi_i} + \frac{d_A - Y_i}{\sin^2 \xi_i} - Y_j + \frac{d_B - X_j}{\tan \xi_j} - \frac{d_B - Y_j}{\sin^2 \xi_j}, \quad (30)$$

set (30) equal to 0, and then solve for d_B to yield:

$$h_\theta = d_B = \frac{\left[Y_i - \frac{d_A - X_i}{\tan \xi_i} + \frac{d_A - Y_i}{\sin^2 \xi_i} - Y_j \right] - \left[\frac{X_j}{\tan \xi_j} + \frac{Y_j}{\sin^2 \xi_j} \right]}{\left[\frac{1}{\tan \xi_j} - \frac{1}{\sin^2 \xi_j} \right]}. \quad (31)$$

For a given visible edge, we consider heights less than h_θ for the fixturing tip B .

Accessibility constraints for B' on the part's the invisible edges can be obtained similarly. Given d_B , $d_{B'}$ and the final orientation of the part, we can then compute the offset between tips along +X-axis (see x_{AB} and $x_{A'B'}$ in Fig. 2) to get the location of the fixturing tips.

B. Form-Closure

We also require that the set of four contacts between the part and the jaw tips generates a form closure grasp.

Let λ denote $[\lambda_1 \lambda_2 \lambda_3 \lambda_4]^T$. We reorder the set of four contacts as (x_1, z_1) , (x_2, z_2) , (x_3, z_3) , and (x_4, z_4) . Let V_k denote the unit normal inward vector at contact (x_k, z_k) , V_{kx} (V_{kz}) denote the X (Z)-axis projection of the vector, and T_k denote the torque of V_k . The wrench matrix is $\mathbf{W} =$

$$\begin{bmatrix} V_{1x} & V_{2x} & V_{3x} & V_{4x} \\ V_{1z} & V_{2z} & V_{3z} & V_{4z} \\ T_1 & T_2 & T_3 & T_4 \end{bmatrix},$$

and the set of contacts achieves a form closure grasp on the part if and only if $\exists \lambda > 0$, s.t. $\mathbf{W}\lambda = \mathbf{0}$.

Given \mathbf{W} , we can determine whether there exists such a λ in time $O(I)$. We compute the 3×3 minors \mathbf{W}_i obtained by removing the i^{th} column from \mathbf{W} . There exists a $\lambda > 0$ satisfying $\mathbf{W}\lambda = \mathbf{0}$ if all the minors \mathbf{W}_i have the same sign and none of them is zero [39]. The four tips achieve a form closure grasp on the part if this condition is satisfied.

VI. ALGORITHM COMPLEXITY

We have given a polynomial-time numerical algorithm to solve the gripper contact problem. An asymptotic upper bound of its running time can be derived as follows.

Given an n -sided polygonal part, we sample its invisible edges to obtain the height of the pushing tip, d_A , and sample its visible edges to obtain the height of the pushing tip, $d_{A'}$. Let k be the number of sample points on each edge.

For each d_A , we construct the corresponding toppling function. Since $\theta_d < \theta_l$, it takes $O(I)$ time to compute each geometric function for a visible edge. There are $O(n)$ visible edges in a graph, so the time to compute each toppling function is $O(n)$. The toppling function allows us to check in time $O(n)$ if a toppling tip at height d_A can rotate the part to the desired orientation with the given pushing tip at height $d_{A'}$. So it takes time $O(n) + O(kn)O(n)$ to find all the feasible d_A for each $d_{A'}$. Therefore, the running time to find all the feasible $(d_A, d_{A'})$ pairs is $O(k^2n^3)$.

Given a pair of feasible $(d_A, d_{A'})$, we apply an $O(n)$ time accessibility analysis to generate the accessible ranges for the fixturing tips. We can then identify the fixturing tips within the accessible ranges in time $O(kn)$. Next we check if each four-contact set achieves form-closure in time $O(I)$. Since there are $O(k^2n^2)$ feasible pairs of $(d_A, d_{A'})$ and there are $O(kn)$ left and right fixturing tips with in the accessible ranges respectively, the algorithm takes time $O(k^4n^4)$ to find the solution or to show no solution exists.

VII. IMPLEMENTATION AND EXPERIMENTS

We implemented our jaw design algorithm as an application using the Java programming language. Mouse input allows a user to draw a part, define its COM and bounds on friction, and select its initial and final orientations; the program then computes and displays the resulting solutions or reports that no solution exists. Fig. 13 illustrate a computed jaw design for the part in Fig. 8, where A at

$(5.93, 95.61)$, A' at $(-6.17, 4.55)$, B at $(42.05, 31.83)$, and B' at $(-21.53, 78.02)$.

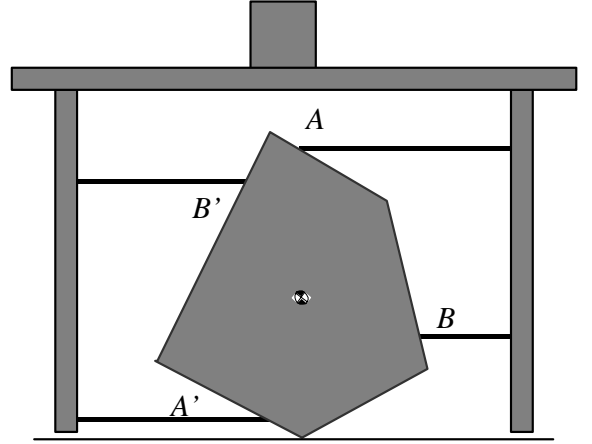


Fig. 13. A resulting jaw design to align the part in Fig. 8.

To explore robustness to initial conditions, we conducted physical experiments using an *AdeptOne* industrial robot and a pneumatic parallel-jaw gripper (*Mecanotron* serial number: 101167) as shown in Fig. 14. The gripper jaws were designed by the algorithm and manually assembled from aluminum stock. To control the velocity of our pneumatic gripper, we added two air regulators (*Wilkerson* serial number: R08-01-F000) and a compression spring (*Century* serial number: C-606).



Fig. 14. Experimental workcell: the robot picks up parts from a convey belt using the parallel-jaw gripper.

The part we used is a small lever from a commercial videotape cassette (*Fuji* serial number: 7410161160). The natural resting pose of the lever is shown in Fig. 15. It must be inserted into a vertical post on the videotape cassette as shown in Fig. 16. Its planar convex hull is shown in Fig. 3. The COM and friction coefficients were determined by physical experiments.



Fig. 15. Natural resting pose of the lever.

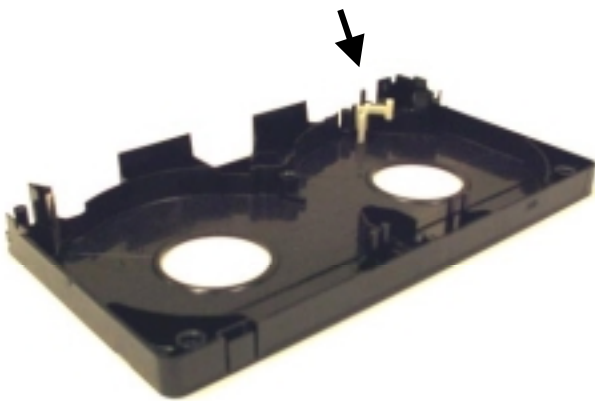


Fig. 16. Assembly: the lever (in white) inserted onto the vertical post.

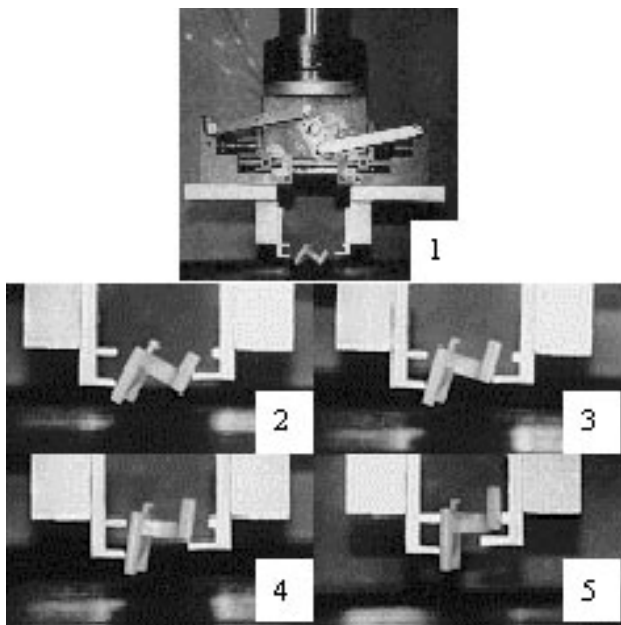


Fig. 17. Part aligning experiment.

Fig. 17 illustrates a successful grasp where the lever rotates in the vertical plane from its resting pose to the

desired orientation $\theta_d = 37^\circ$. The part begins in stable orientation in (1). Its desired orientation for insertion is (5). We choose A and A' at $d_A = 6\text{mm}$ and $d_{A'} = 5\text{mm}$, respectively. The friction cone bounds are $\alpha_l = [0, 5^\circ]$ and $\alpha_s = [0, 10^\circ]$. When $\theta < 37^\circ$, P is v_1 and $x_2 = 14\text{mm}$, $z_2 = 0\text{mm}$, $\psi_2 = 56^\circ$, $\eta = 46^\circ$, $\rho = 7\text{mm}$, and $\omega = 53^\circ$; When $\theta > 37^\circ$, P is v_6 and $x_2 = 16\text{mm}$, $z_2 = 8\text{mm}$, $\psi_2 = 92^\circ$, $\eta = 55^\circ$, $\rho = 9\text{mm}$, and $\omega = 89^\circ$. For $k = 10$, the algorithm requires approximately one second on a 233MHz Pentium II PC running Microsoft J++ 6.0 to find 43 solutions. The gripper jaws in Fig. 17 have the following contact values: $d_B = 11\text{mm}$, $d_{B'} = 13\text{mm}$, $x_{AB} = 5\text{mm}$, and $x_{A'B'} = 1\text{mm}$.

We conducted two experiments to test sensitivity.

In Experiment 1, we tested the gripper 50 times at each of seven height offsets. The results are shown in Fig. 18. All 50 trials were successful at the nominal gripper height (offset = 0). But grasping is sensitive to small variations in gripper height; the part can jam in the gripper or be ejected when the gripper height is offset.

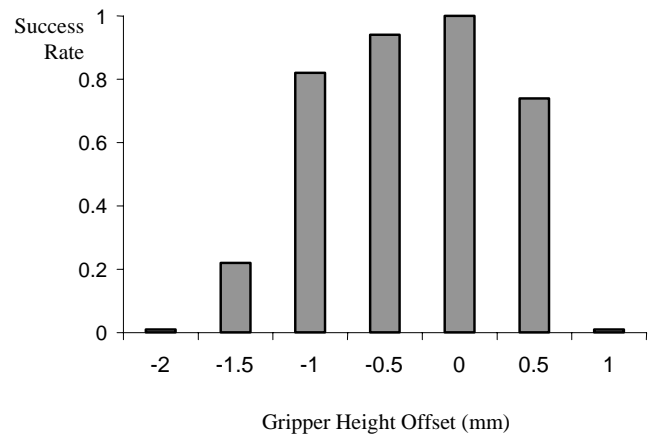


Fig. 18. Success rate when the height of the gripper varies (50 trials each offset).

In Experiment 2, we vary gripper angle. Fig. 19 illustrates a top view of the part (in gray) and the gripper jaws (in black). The arrows indicate the motion direction of jaws: δ is the angular error.

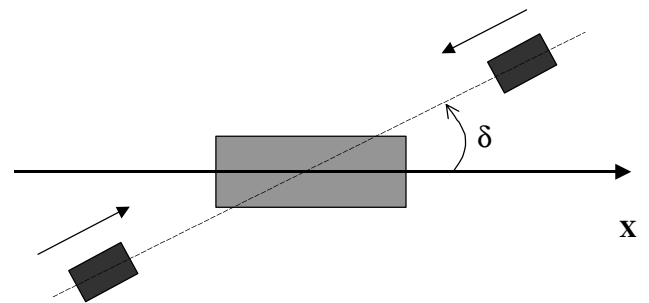


Fig. 19. Top view: Error in gripper angle δ .

Fig. 20 shows that all 50 trials are successful even when the gripper is rotated by $\pm 10^\circ$. Grasping can fail for larger rotations, where the part is ejected or causes the gripper to jam.

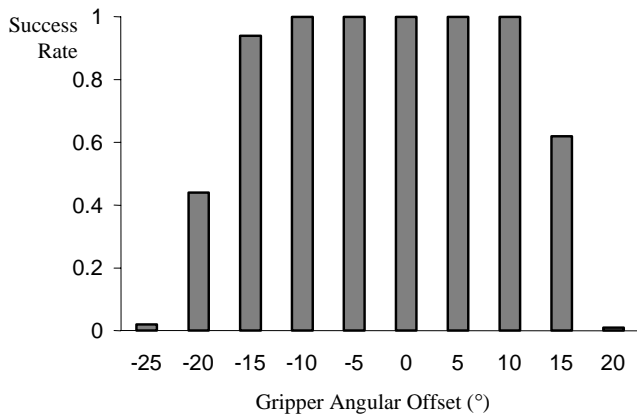


Fig. 20. Success rate when the angle of the gripper varies (50 trials each offset).

VIII. DISCUSSION AND FUTURE WORK

Designing gripper jaws is particularly challenging when the natural resting pose of a part differs from the pose desired for insertion. In this paper we consider a minimalist solution where four contact tips on a parallel-jaw gripper guide the part into alignment and hold it securely. We analyze the gripper contact design problem based on a geometric analysis of the mechanics of toppling, jamming, accessibility, and form closure and give a polynomial-time numerical algorithm.

In future work we will extend our analysis to other geometric contact models and study the conditions under which solutions are guaranteed to exist.

ACKNOWLEDGEMENTS

This paper grew out of practical experiments with a commercial assembly. We would like to thank Brian Carlisle from Adept Technology, Inc. and Randy Brost from Eastman Kodak Co. for suggesting these experiments and Kevin Lynch from Northwestern Univ. for his elegant toppling analysis. We would also like to thank Robert-Paul Beretty from UNC Chapel Hill, and A. Frank van der Stappen and Mark Overmars from Utrecht Univ. for their contributions to our thinking about the toppling function and Gordon Smith for suggesting that toppling could be applied to grasping. Thanks also to K. “Gopal” Gopalakrishnan and Yong Liu, and Mark Moll from Carnegie Mellon Univ., and Peng Song and Vijay Kumar from the Univ. of Pennsylvania for helpful discussions. We also thank the anonymous reviewers of an earlier version of this paper for their constructive feedback. This work was supported in part by the National Science Foundation under DMI-0010069, CDA-9726389 and Presidential Faculty Fellow Award IRI-9553197. Research funding was also provided by Adept Technology, Inc., Ford Motor Co., and California State MICRO Grant 00-032.

REFERENCES

[1] T. Abell and M. Erdmann, “Stably supported rotations of a planar polygon with two frictionless Contacts,” in *Proc.*

IEEE/RSJ Int. Conf. Intell. Robots Syst., Pittsburgh, PA, 1995, pp. 411-8.

[2] S. Akella, W. Huang, K. Lynch, and M. Mason, “Parts feeding on a conveyor with a one joint robot,” *Algorithmica*, vol. 26, no. 3-4, pp. 313-44, 2000.

[3] A. Bicchi and V. Kumar, “Robotic grasping and contact: a review,” in *Proc. IEEE Int. Conf. Robot. Automat.*, San Francisco, CA, 2000, pp. 348-353.

[4] A. Bicchi, “Hands for dexterous manipulation and robust grasping: a difficult road toward simplicity,” *IEEE Trans. Robot. Automat.*, vol. 16, no. 6, pp. 652-62, 2000.

[5] S. Blind, C. McCullough, S. Akella, and J. Ponce, “A reconfigurable parts feeder with an array of pins,” in *Proc. IEEE Int. Conf. Robot. Automat.*, San Francisco, CA, 2000, pp. 147-53.

[6] R. Brost, “Automatic grasping planning in the presence of uncertainty,” *Int. J. Robot. Automat.*, vol. 7, no. 1, pp. 3-17, 1988.

[7] R. Brown and R. Brost, “A 3-D modular gripper design tool,” *IEEE Trans. Robot. Automat.*, vol. 15, no. 1, pp. 174-86, 1999.

[8] G. Causey and R. Quinn, “Gripper design guidelines for modular manufacturing,” in *Proc. IEEE Int. Conf. Robot. Automat.*, Leuven, Belgium, 1998, pp. 1453-8.

[9] M. Erdmann and M. Mason, “An exploration of sensorless manipulation,” *IEEE J. Robot. Automat.*, vol. 4, no. 4, pp. 369-79, 1988.

[10] M. Erdmann, “An exploration of nonprehensile two-palm manipulation,” *Int. J. Robot. Res.*, vol. 17, no. 5, pp. 485-503, 1998.

[11] K. Goldberg, “Orienting polygonal parts without sensors,” *Algorithmica*, vol. 10, no. 2, pp. 201-25, 1993. Special Issue on Computational Robotics.

[12] K. Goldberg, B. Mirtich, Y. Zhuang, J. Craig, B. Carlisle, and J. Canny, “Part pose statistics: estimators and experiments,” *IEEE Trans. Robot. Automat.*, vol. 15, no. 5, pp. 849-57, 1999.

[13] R. Grupen, T. Henderson, and I. McCammon, “A survey of general-purpose manipulation,” *Int. J. Robot. Res.*, vol. 8, no. 1, pp. 38-62, 1989.

[14] L. Han, J. Trinkle, and Z. Li, “Grasp analysis as linear matrix inequality problems,” *IEEE Trans. Robot. Automat.*, vol. 16, no. 6, pp. 663-74, 2000.

[15] W. Hessler, “How to build simple, effective pick-and-place devices,” *Robot Today*, vol. 9, no. 4, pp. 1-5, 1996.

[16] R. Howe and M. Cutkosky, “Touch sensing for robotic manipulation and recognition,” in *Robot. Rev. 2*, Khatib, Ed., Cambridge, MA: MIT Press, 1992.

[17] M. Kaneko, K. Harada, and T. Tsuji, “A sufficient condition for manipulation of envelope family,” in *Proc. IEEE Int. Conf. Robot. Automat.*, San Francisco, CA, 2000, pp. 1060-7.

[18] Y. Liu, “Computing n -finger form closure grasps on polygonal objects,” *Int. J. Robot. Res.*, vol. 19, no. 2, pp. 149-58, 2000.

[19] K. Lynch, “Toppling manipulation,” in *Proc. IEEE Int. Conf. Robot. Automat.*, Detroit, MI, 1999, pp. 2551-7.

[20] K. Lynch, “Inexpensive conveyor-based parts feeding,” *Assembly Automat.*, vol. 19, no. 3, pp. 209-15, 1999.

[21] X. Markenscoff, L. Ni and C. Papadimitriou, “The geometry of grasping,” *Int. J. Robot. Res.*, vol. 9, no. 1, pp. 61-74, 1990.

[22] M. Mason and J. Salisbury, *Robotic Hands and the Mechanics of Manipulation*. Cambridge, MA: MIT Press, 1985.

[23] M. Mason, “Two graphical methods for planar contact problems,” in *Proc. IEEE/RSJ Int. Workshop Intell. Robots Syst.*, Osaka, Japan, 1991, pp. 443-8.

[24] B. Mishra, J. Schwartz, and M. Sharir, “On the existence and synthesis of multifinger positive grips,” *Algorithmica*, vol. 2, no. 4, pp. 541-58, 1987.

[25] M. Moll and M. Erdmann, “Manipulation of pose distributions,” in *Algorithmic and Computational Robotics: New Directions*, B. Donald, K. Lynch, and D. Rus, Eds., Natick, MA: A K Peters, 2001, pp. 127-41.

[26] R. Murray, Z. Li, and S. Sastry, *A Mathematical Introduction to Robotic Manipulation*. Boca Raton, FL: CRC, 1994.

[27] A. Okamura, N. Smaby, and M. Cutkosky, “A overview of dexterous manipulation,” in *Proc. IEEE Int. Conf. Robot. Automat.*, San Francisco, CA, 2000, pp. 255-62.

- [28] J. Ponce, S. Sullivan, A. Sudsang, J.-D. Boissonnat, and J.-P. Merlet, "On computing four-finger equilibrium and force closure grasps of polyhedral objects," *Int. J. Robot. Res.*, vol. 16, no. 1, pp. 11-35, 1997.
- [29] H. Qiao and S. Tso, "Three-step precise robotic peg-hole insertion operation with symmetric regular polyhedral objects," *Int. J. Production Res.*, vol. 37, no. 15, pp. 3541-63, 1999.
- [30] H. Qiao, "Attractive regions formed by constraints in configuration space," in *Proc. IEEE Int. Conf. Robot. Automat.*, Seoul, Korea, 2001, pp. 1071-8.
- [31] A. Rao, D. Kriegman and K. Goldberg, "Complete algorithm for feeding polyhedral parts using pivot grasps," *IEEE Trans. Robot. Automat.*, vol. 12, no. 2, pp. 331-42, 1996.
- [32] E. Rimon and J. Burdick, "Mobility of bodies in contact-part I: a 2nd-order mobility index for multiple-finger grasps," *IEEE Trans. Robot. Automat.*, vol. 14, no. 5, pp. 696-708, 1998.
- [33] K. Shimoga, "Robot grasp synthesis algorithms: a survey," *Int. J. Robot. Res.*, vol. 15, no. 3, pp. 230-66, 1996.
- [34] A. F. van der Stappen, C. Wentink, and M. Overmars, "Computing immobilizing grasps of polygonal parts," *Int. J. Robot. Res.*, vol. 19, no. 5, pp. 467-79, 2000.
- [35] P. Song, M. Yashima, and V. Kumar, "Dynamic simulation for grasping and whole arm manipulation," in *Proc. IEEE Int. Conf. Robot. Automat.*, San Francisco, CA, 2000, pp. 1082-7.
- [36] J. Trinkle, J. Abel, and R. Paul, "Enveloping frictionless planar grasping," in *Proc. IEEE Int. Conf. Robot. Automat.*, San Francisco, CA, 1987, pp. 246-51.
- [37] J. Trinkle and R. Paul, "Planning for dexterous manipulation with sliding contacts," *Int. J. Robot. Res.*, vol. 9, no. 3, pp. 24-48, 1990.
- [38] J. Trinkle, "On the stability and instantaneous velocity of grasped frictionless objects," *IEEE Trans. Robot. Automat.*, vol. 8, no. 5, pp. 560-72, 1992.
- [39] A. Wallack and J. Canny, "Planning for modular and hybrid fixtures," *Algorithmica*, vol. 19, pp. 40-60, 1997.
- [40] Y. Yu, K. Fukuda, and S. Tsujio, "Estimation of mass and center of mass of grasplless and shape-unknown object," in *Proc. IEEE Int. Conf. Robot. Automat.*, Detroit, MI, 1999, pp. 2893-8.
- [41] R. Zhang and K. Gupta, "Automatic orienting of polyhedral through step devices," in *Proc. IEEE Int. Conf. Robot. Automat.*, Leuven, Belgium, 1998, pp. 550-6.
- [42] T. Zhang, G. Smith, R. Berretty, M. Overmars, and K. Goldberg, "The toppling function: designing pin sequences for part feeding," in *Proc. IEEE Int. Conf. Robot. Automat.*, San Francisco, CA, 2000, pp. 139-46.
- [43] T. Zhang, G. Smith, and K. Goldberg, "Compensatory grasping with the parallel-jaw gripper," in *Proc. 4th Int. Workshop Algorithmic Foundations of Robot.*, Hanover, NH, 2000, pp. FR27-37.
- [44] N. Zumel and M. Erdmann, "Nonprehensile two palm manipulation with non-equilibrium transitions between stable states," in *Proc. IEEE Int. Conf. Robot. Automat.*, Minneapolis, MN, 1996, pp. 3317-23.
- [45] N. Zumel and M. Erdmann, "Nonprehensile manipulation for orienting parts in the plane," in *Proc. IEEE Int. Conf. Robot. Automat.*, Albuquerque, NM, 1997, pp. 2433-9.